ELSEVIER

Catalysis Today 44 (1998) 101–109

CATALYSIS TODAY

# MCM-48 supported chromium catalyst for trichloroethylene oxidation

S. Kawi*, M. Te

*Department of Chemical Engineering, National University of Singapore, 10 Kent Ridge Crescent, Singapore 119260, Singapore*

**Abstract**

MCM-48 supported chromium (Cr/MCM-48) catalyst was prepared by introduction of chromium chloride during gel-preparation for the hydrothermal synthesis of MCM-48. Based on the $N_2$ adsorption/desorption isotherm, BET, pore size distribution, XRD, FTIR, TGA, and DTA data, Cr/MCM-48 was found to have high surface area (~832 $m^2$/g), uniform pore size distribution (~24 Å), mesoporous structures similar to MCM-48 itself, and incorporation of about 3 wt% of Cr component in the mesoporous framework. Cr/MCM-48 was very active for the oxidative destruction of trichloroethylene (TCE), which is a typical chlorinated volatile organic compound (CVOC); 100% conversion of TCE was achieved at 350°C. Based on the TGA of trichloroethylene/water adsorption study, it was found that MCM-48 had high adsorption capacity (>0.25 g TCE/g catalyst). In addition, the hydrophobicity of the adsorptive properties of Cr/MCM-48 materials could be modified. The high adsorption capacity and catalytic activity of Cr/MCM-48 material make it suitable for adsorption/catalysis bifunctional systems for energy-saving treatment of low concentration of VOC or CVOC. 

*Keywords:* MCM-48; Transition metal catalysts; Chlorinated VOC (CVOC); Trichloroethylene (TCE); Surfactant template

## 1. Introduction

Catalytic oxidative destruction of chlorinated volatile organic compounds (CVOC) has gained interest recently as one of the important treatment strategies for environmental protection. Since the concentration of CVOC in an industrial gas stream is usually low, research interest is being focused recently on the development of porous materials having both adsorptive and catalytic properties. The sorption/catalysis bifunctional process could provide a highly energy efficient cyclic process for the destruction of low concentration of CVOCs in an industrial gas stream. For example, Greene and coworkers [1–4] developed a combined sorbent/catalyst system using transition metal exchanged zeolites for the adsorption/destruction of gas streams containing low concentration trichloroethylene (TCE, 1000 ppm) or methylene chloride ($CH_2Cl_2$, 1000 ppm). They showed that a Cr/ZSM-5 sorbent/catalyst system had a sorption capacity of 0.074 g TCE (or 0.064 g $CH_2Cl_2$)/g sorbent at 23°C, and more than 95% of the adsorbed TCE or the adsorbed $CH_2Cl_2$ could be oxidatively destructed at 300°C.

A chromium oxide loaded Ambersorb adsorbent was also shown to be effective for the destruction of high concentration $CH_2Cl_2$ (60 000 ppm) at low temperature (250°C) [5,6]; however, the relatively low gas hourly space velocity was a limiting factor for the

*Corresponding author. Tel.: 00 65 874 6312; fax: 00 65 779 1936; e-mail: chekawis@nus.sg

0920-5861/98/$32.00 
*PII* S0920-5861(98)00178-3

system. Lately, chromium (oxide) supported on pillared clay [7], sulfated oxides [8], $SnO_2$ [9], and zeolites [10] were also found to be active for CVOC destruction, indicating that chromium was playing the major role as active catalytic sites and the other components are primarily serving as supporting media or promoters.

Since the M41S family of mesoporous materials were discovered by Mobil researchers in 1992 [11], they have widely been studied for various adsorptive and catalytic applications. However, the investigation of M41S mesoporous materials for catalytic destruction of CVOCs has not been reported up to date. It is strongly believed that M41S materials should have great potentials as adsorbents and catalysts for the destruction of CVOC due to their high surface area (>1000 $m^2$/g), large, unique and tunable pore size (15–100 Å), large pore volume, framework incorporation of transition metals, and high thermal stability.

This paper reports the preliminary results of the synthesis, characterization, and catalytic application of Cr/MCM-48 catalysts for the oxidative destruction of trichloroethylene.

## 2. Experimental

### 2.1. Catalyst synthesis

Using slight modification of the synthesis procedure reported by Schmidt et al. [12], MCM-48 was synthesized as follows. 14.9 g of $C_{19}H_{42}BrN$ (*N*-Cetyl-*N*,*N*,*N*-trimethylammonium bromide, Merck) was added to a container containing 21.3 g of TEOS (tetraethoxysilane, >98%, Strem Chemicals), 2.48 g of NaOH (sodiumhydroxide anhydrous, >99%, SINO Chemicals), and 180.2 g of deionized $H_2O$. The solution mixture was preheated in a water bath kept at 36°C, and was stirred at 500 rpm for 5 min. After stirring, 1.1 g of $Al_2(SO_4)_3{\cdot}18H_2O$ (Riedel-DE Haen AG Seelze-Hannover) was added to the solution mixture. The solution mixture was then stirred further for 55 min. The resultant gel was loaded to three 100 ml Teflon-lined autoclaves, and the mixture was hydrothermally treated at 100°C for 72 h. The mixture was then filtered and washed with 500 ml deionized $H_2O$. The washing procedure was repeated 5–6 times to assure the complete removal of the bromide and other free ions. The solid was dried at 50°C for overnight. The dried solid was then calcined in air at 600°C (using a heating rate of 1°C/min) for 600 min.

Cr/MCM-48 catalyst was prepared by the introduction of chromium chloride during the gel-preparation followed by the similar treatment as applied to MCM-48. The Si/Al/Cr ratio of Cr/MCM-48 was set to be 30/1/1, resulting in about 3 wt% of Cr in the catalyst.

Cr/Si-MCM-48 (i.e. Cr supported on pure silica Si-MCM-48) was prepared similarly as above, except that aluminum was not included in the starting gel.

### 2.2. Catalyst characterization

Nitrogen adsorption/desorption isotherms, BET surface areas, and BJH (Barrett, Joyner and Halenda) pore size distributions of the calcined catalysts were determined at 77 K on a NOVA-1000 gas sorption analyzer (Quantachrome) using a continuous adsorption procedure.

X-ray diffraction patterns of the catalysts were determined on a Shimadzu XRD-6000 X-ray diffractometer using Cu $K_\alpha$ radiation ($\lambda$=1.5418) and a scan speed of 2° $min^{-1}$ at 40 kV and 30 mA.

Pyridine adsorption of the calcined catalysts was studied on a Shimadzu Fourier transform infrared spectrophotometer (FTIR-8101 M with 2 $cm^{-1}$ resolution) using an in situ IR cell made of quartz with $CaF_2$ windows.

Thermogravimetry analysis/differential thermal analysis (TGA/DTA) of the catalysts were carried out on a Shimadzu DTG-50 simultaneous DTA-TG thermal analysis system.

### 2.3. Adsorption study

TCE/water adsorption study was performed based on thermogravimetric analysis using a Shimadzu DTG-50 thermal analysis system; this TGA system was equipped with an organic vapor accessory which could be used to feed a certain concentration of TCE or water vapor into the TGA analysis system. The adsorption study was carried out by: (1) degassing the sample in a 20 ml/min purified air or oxygen gas stream by heating the sample from RT to 400°C at a ramping rate of 20°C/min, (2) cooling the sample to

RT in the same gas flow, (3) feeding certain concentration (e.g. 34 000 ppm) of TCE through the organic vapor accessory, and (4) measuring the weight increase (due to the adsorption of TCE on the sample) until saturation.

The adsorption of water on the sample was determined similarly as the TCE adsorption described above. The effect of pre-adsorbed water on the adsorption of TCE was also examined by doing sequential adsorption of water followed with TCE.

It should be pointed out that there might be some limitation in the adsorption study using TGA. In the TGA adsorption study, the sample was held in a small sample holder and the adsorption was achieved mainly by diffusion. Hence the data obtained might not be quantitatively comparable to those determined in a fixed bed flow system; however they still give a good qualitative understanding on the effect of chemical composition and physical structures of the materials on the adsorption of organic vapors in the presence of water vapor.

### 2.4. Catalytic testing

The oxidative destruction of TCE was performed using 0.20 g of Cr/MCM-48 catalyst loaded in a tubular glass reactor (i.d. 8 mm, 350 mm in length) and the reaction was performed at 250–400°C using oxygen as the oxidant. The TCE concentration used in the reaction was set at 34 000–60 000 ppm, and the flow rate of the mixture was maintained at 15 ml/min.

The reaction product was monitored by an on-line HP-6890 gas chromatograph, which is equipped with a flame ionization detector (FID), an HP-5 (cross-linked 5% PH ME siloxane) capillary column (0.25 μm film thickness, 0.32 mm internal diameter, and a length of 30 m) and an auto sampling system. The reactor effluent was passed through a solid NaOH trap to avoid the corrosive components, such as HCl, from getting into the GC system.

Based on the GC analysis of the products, there were no CVOCs other than TCE observed, suggesting that the destruction of TCE was complete. The destruction products were likely to be a range of inorganic components, such as $CO_2$, CO, HCl, $Cl_2$, $COCl_2$ and $H_2O$ (to be determined in the future work).

## 3. Results and discussion

### 3.1. Catalyst characterization

Table 1 shows that Cr/MCM-48 has high surface area (832 $m^2/g$), which seems to be lower than MCM-48 (1034 $m^2/g$), or the original MCM-48 reported in [12]. As it is generally expected that the introduction of transition metals onto the mesoporous M41S materials would result in a decrease of the surface area, the slightly lower surface area of Cr/MCM-48 may be attributed to the incorporation of heavy element Cr in the framework.

Fig. 1 shows the nitrogen adsorption/desorption isotherms of Cr/MCM-48, with sharp increase in the adsorbed volume of $N_2$ between $P/P_0$=0.25–0.35. The sharp increase in both isotherms is indicative of Kelvin condensation in the framework confined mesopores having an average pore size of 24 Å. The observed isotherms of Cr/MCM-48 are typical for

Table 1
Physical properties of the materials

| Catalysts | Surface area ($m^2/g$) | Pore size (Å) |
|---|---|---|
| MCM-48 | 1034 | 27 |
| Cr/MCM-48 | 832 | 24 |
| Used Cr/MCM-48 | 825 | 22 |
| Cr/Si-MCM-48 | 982 | 23 |

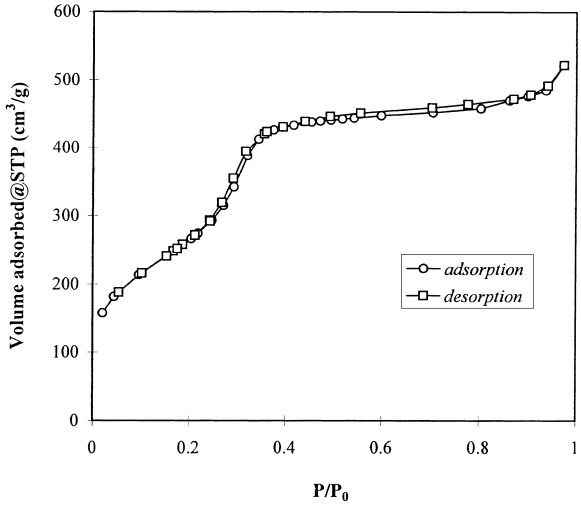


Fig. 1. $N_2$ adsorption/desorption isotherms of Cr/MCM-48.

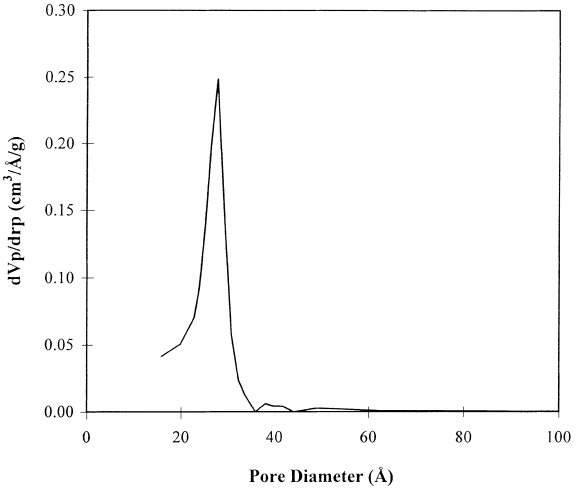


Fig. 2. Pore size distribution of Cr/MCM-48.

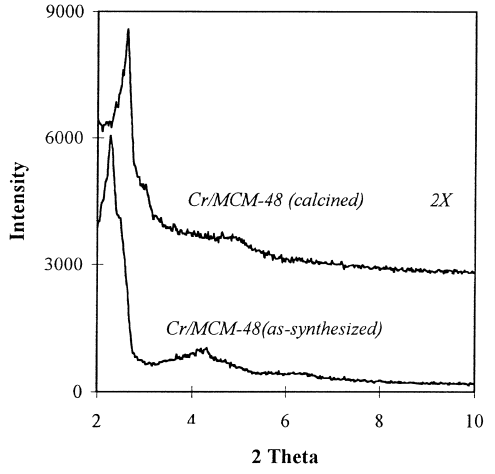


Fig. 3. XRD of as-synthesized and calcined Cr/MCM-48.

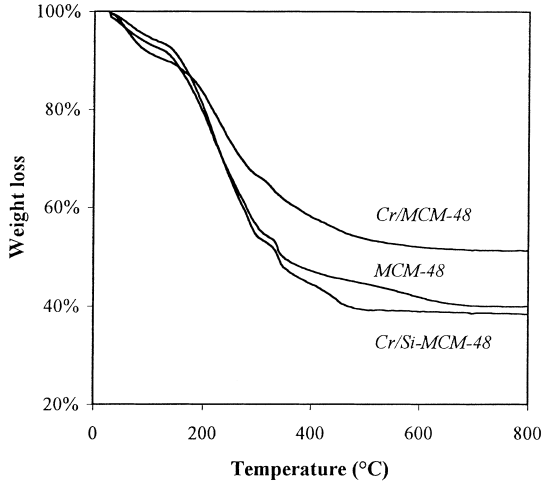


Fig. 4. TGA plots of MCM-48, Cr/MCM-48 and Cr/Si-MCM-48.

mesoporous M41S materials reported in literatures. MCM-48 and Cr/Si-MCM-48 also showed quite similar adsorption/desorption isotherms as those shown in Fig. 1. The adsorption/desorption isotherm results indicate that the loading of a significant amount (∼3 wt%) of Cr component onto MCM-48 does not lead to any detrimental changes of the mesoporous structure of MCM-48.

The BJH pore size distribution for Cr/MCM-48, as shown in Fig. 2, exhibits a narrow pore size distribution centered at 24 Å, indicating that the mesopores of Cr/MCM-48 are very uniform. Table 1 shows that the average pore size of Cr/MCM-48 (24 Å) is a little bit smaller than that of MCM-48 (27 Å), further suggesting that the larger Cr element (3 wt%) may have been incorporated in the framework, causing the pore size to be slightly decreased.

The mesoporous structure of the catalysts has been further confirmed by XRD characterization results. For example, the XRD patterns of the as-synthesized and calcined Cr/MCM-48 (Fig. 3) are consistent with those reported for MCM-48 [12], indicating that the cubic mesoporous structures of MCM-48 have been maintained in Cr/MCM-48. A lattice contraction upon calcination of the sample in air was observed from the increased 2-theta value of the major XRD diffraction at low 2-theta angle. The XRD data also reveal that there is no significant metal oxide XRD signatures for Cr/MCM-48, indicating that Cr components are highly dispersed and possibly were structurally incorporated in the framework.

Fig. 4 shows the TGA plots of weight loss observed during calcination of MCM-48, Cr/MCM-48, and Cr/Si-MCM-48 materials. All the samples showed typical weight loss patterns in the TGA plots as reported in the literature for M41S materials [13]. The weight loss can be attributed to happen in two stages: (1) the removal of the template associated with Si–O (silanol groups) at temperatures below 350°C, and (2) the removal of the template associated with aluminum (Al–O) (and other metal components) at temperatures between

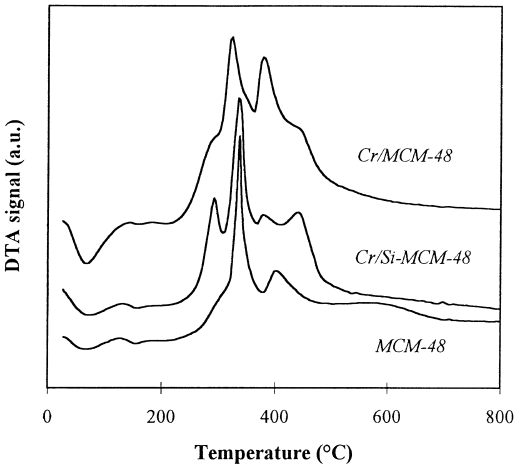


Fig. 5. DTA plots of MCM-48, Cr/MCM-48 and Cr/Si-MCM-48.

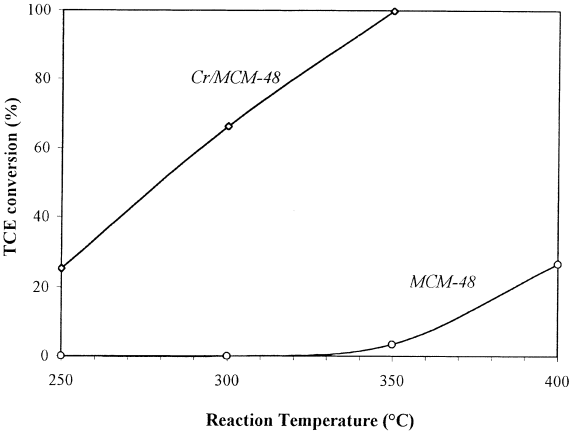


Fig. 6. TCE conversions of MCM-48 and Cr/MCM-48 catalysts as a function of reaction temperature (performed using 60 000 ppm TCE).

350°C and 600°C. Corresponding to their compositions, the first stage surfactant removal accounts for the major weight loss. The relative weight loss observed for the two stages together is typically about 50%, which corresponds well with the initial composition of the starting gel. There are additional features on the TGA curves of MCM-48 supported Cr catalysts (i.e. Cr/MCM-48 and Cr/Si-MCM-48), which may indicate the interactions between the incorporated Cr components and the templated surfactant molecules.

The DTA plots of the calcination of catalysts, as shown in Fig. 5, can be used to identify the fine metal–template interactions indicated in TGA plots. The major exothermic DTA peak observed at temperatures below 350°C is due to the oxidation of the surfactant templates associated to silanol groups. The exothermic DTA peaks observed at temperatures above 350°C are suggested to be due to the oxidation of the surfactant templates associated to Al and Cr that were present in wall materials. Interestingly, comparing the DTA plots of Cr/MCM-48 and Cr/Si-MCM-48 with those of MCM-48, an extra exothermic DTA peak could be observed at around 450°C on the MCM-48 supported chromium catalysts. These results show that there may be direct interactions between the templated surfactant molecules with chromium, indicating the incorporation of chromium into the wall material.

Although the adsorption/desorption isotherms, pore size distribution, XRD, TGA, and DTA data may have pointed out the incorporation of Cr in the framework of MCM-48, however it should be pointed out that some other techniques, such as solid state NMR, need to be employed to confirm this observation.

### 3.2. *Catalyst performance on oxidative destruction of TCE*

Catalytic oxidative destruction of TCE was performed in order to explore the environmental applications of Cr/MCM-48 catalysts. Fig. 6 shows the catalytic conversion of TCE of the catalysts at different temperatures. Cr/MCM-48 exhibited superior performance for TCE destruction; in fact, it could completely destroy TCE at 350°C. At this temperature, MCM-48 catalyst could only destruct less than 5% of TCE.

Furthermore, Fig. 7 displays the excellent catalytic stability of Cr/MCM-48 catalyst in an extended period (72 h) of reaction test; the BET surface area of the Cr/MCM-48 catalyst was unchanged after the prolonged reaction (see Table 1).

Fig. 8 shows the pyridine-adsorption infrared spectra of the catalysts. It is interesting to note here that, although both MCM-48 and Cr/MCM-48 catalysts showed significant Brønsted acidity and Lewis acidity, however Cr/MCM-48 was very active for oxidative destruction of TCE while MCM-48 catalyst was not so active. The result shows that the presence of Cr (not the acidity) is playing the major role in the catalytic

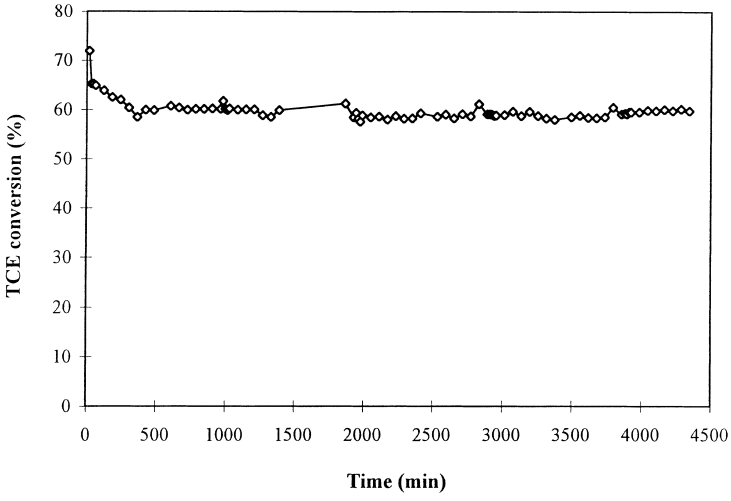


Fig. 7. Catalytic stability of Cr/MCM-48 at 300°C (performed using 60 000 ppm TCE).

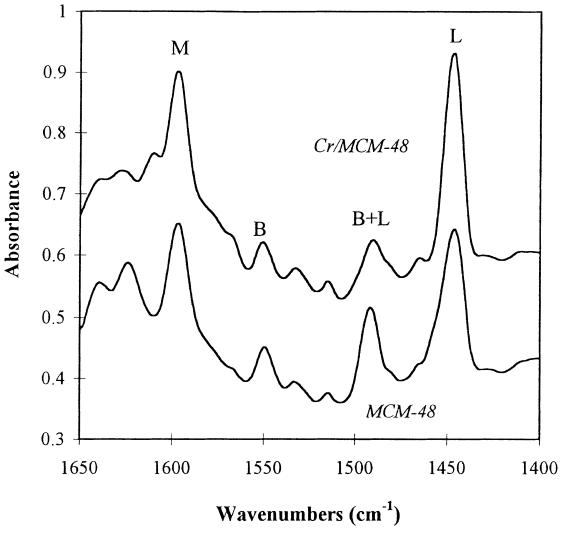


Fig. 8. Pyridine-adsorption infrared data of MCM-48 and Cr/MCM-48 (measured under vacuum at 200°C, L=Lewis acid site, B=Brønsted acid sites, M=molecularly adsorbed site).

destruction of TCE. In fact, chromium (oxide) catalysts supported on various media, including zeolite [1–3], Ambersorb adsorbent [5,6], pillared clay [7], and $SnO_2$ [9] reported in the literature, as well as MCM-48 reported in this paper, all displayed excellent activity for the oxidative destruction of TCE. Therefore, it is likely that the nature of the active site of chromium (oxide) itself (such as its low ionization potential and the availability of its high oxidation state) is playing the key role in the catalysis, and the supporting media mainly provide the stable and high dispersion of the active components.

### 3.3. *Effect of water vapor on catalytic activity*

As the water vapor in a gas stream competes with CVOC for adsorption and active sites, it is important to investigate the effect of water on the activity of the catalysts for the oxidative destruction of CVOC. It was reported that the CVOC adsorption capacity and the CVOC destruction activity of various catalysts are generally decreased upon contacting with a high concentration of water vapor in the gas stream [2,3,8], although a low concentration of water vapor is sometimes helpful for complete destruction of hydrogen lean CVOC, for example, $CCl_4$.

Fig. 9 shows the effect of water vapor on the catalytic activity of the MCM-48 supported chromium catalysts for the destruction of TCE. The result shows that a high concentration of water vapor (8000 ppm) in the gas stream is detrimental to the catalytic activity of Cr/MCM-48 catalysts, whereas a lower concentration of water vapor (1000 ppm) in the gas stream has negligible influence on the catalytic activity of the Cr/MCM-48 catalyst. The result also shows that, although the Cr/Si-MCM-48 catalyst showed quite similar stable activity at the low concentration of

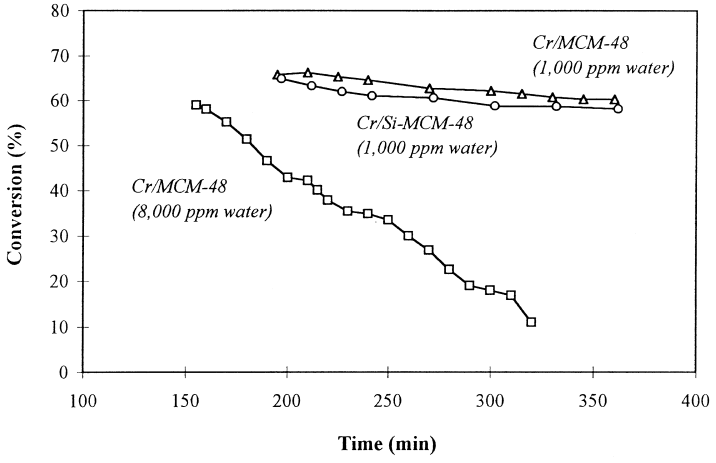


Fig. 9. Effect of water vapor on the catalytic activities of the catalysts at 350°C (performed using 34 000 ppm TCE).

water vapor in the gas stream, however Cr/Si-CM-48 catalyst had significantly higher TCE adsorption and hydrophobicity compared to Cr/MCM-48, as discussed below.

### 3.4. Effect of water on TCE adsorption

It was found that water adsorption on the zeolite catalysts leads to significant decreases of TCE adsorption capacity of the materials [2,3]. However, Drago and coworkers [5,6] found that high concentration water did not lead to any deactivation for those Ambersorb absorbent and Ambersorb absorbent supported catalysts, which, apparently, could be attributed to the intrinsic hydrophobic features of the Ambersorb absorbent.

Accordingly, to improve the water tolerance of the Cr/MCM-48 catalyst, it is essential to modify the surface property of MCM-48 to make it more hydrophobic. For this purpose, a pure silica MCM-48 (i.e. Si-MCM-48) supported chromium catalyst was developed. The removal of aluminum from the system should, presumably, enhance the hydrophobicity of the material because aluminum site in the framework is normally thought to be responsible for the hydrophilic behavior while silica surface is more hydrophobic in nature. To compare the water/TCE adsorption properties, Cr/MCM-48 and Cr/Si-MCM-48 were subjected to water/TCE adsorption study using TGA.

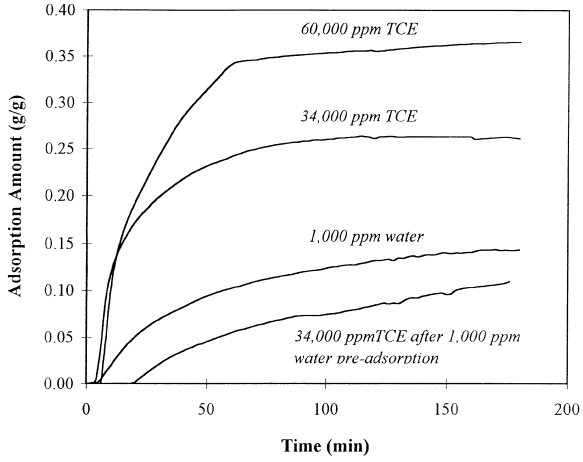


Fig. 10. Effect of water preadsorption on TCE adsorption on Cr/MCM-48 at 25°C.

Figs. 10 and 11 show the TGA plots of the TCE/water adsorption on Cr/MCM-48 and Cr/Si-MCM-48 catalysts, respectively. The results of Figs. 10 and 11 are summarized in Table 2. Several points can be drawn from these results: (1) Both Cr/MCM-48 and Cr/Si-MCM-48 catalysts showed high TCE adsorption capacity; for an example, at 34 000 ppm TCE level, they adsorb 0.26 and 0.52 g TCE/g catalyst, respectively. (2) The adsorption capacity of the catalysts is dependent on the concentration (partial pressure) of TCE; the higher the partial

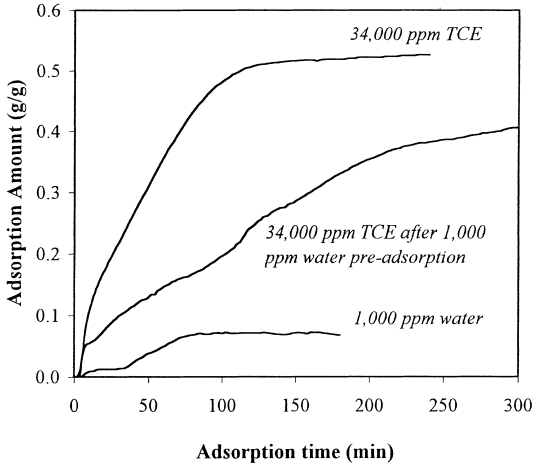


Fig. 11. Effect of water preadsorption on TCE adsorption on Cr/Si-MCM-48 at 25°C.

Table 2
TCE, water, and effect of water on TCE adsorption on catalysts (g/g)

| | Cr/MCM-48 | Cr/Si-MCM-48 |
|---|---|---|
| TCE (60 000 ppm) | 0.40 | — |
| TCE (34 000 ppm) | 0.26 | 0.52 |
| Water (1000 ppm) | 0.14 | 0.06 |
| TCE (34 000 ppm) (after 1000 ppm water preadsorption) | 0.12 | 0.42 |

pressure of TCE, the more TCE can be adsorbed. (3) The Cr/Si-MCM-48 catalyst showed much higher TCE adsorption compared to Cr/MCM-48, indicating the hydrophobicity of the surface property of Cr/Si-MCM-48. (4) Water adsorption data clearly indicated that Cr/MCM-48 is more hydrophilic than Cr/Si-MCM-48, which is consistent with TCE adsorption and reaction results mentioned above, and consequently, (5) water pre-adsorbed Cr/Si-MCM-48 showed much higher TCE adsorption than Cr/MCM-48 (0.42 g/g versus 0.12 g/g).

To compare the TCE adsorption on zeolite Y to those on MCM-48 supported chromium catalysts, a zeolite Y sample was tested in the TCE adsorption study using 34 000 ppm TCE as the adsorbate. Only about 0.01 g TCE/g zeolite Y adsorption was observed by TGA in the timescale used for above mentioned experiments, showing that the MCM-48 supported catalysts have about 25–50 times more adsorption capacity than zeolite Y.

Although chromium-exchanged zeolites [1–3] and Ambersorb adsorbent supported $Cr_2O_3$ [5,6] have been reported to be very active for the oxidative destruction of CVOCs, the newly developed Cr/MCM-48 catalysts offer much larger surface area and pore size or pore volume, and therefore they should offer less diffusion restrain and higher adsorption capacity. While MCM-48 supported catalysts have similar surface area as the Ambersorb adsorbent catalysts, the thermal stability and the very narrow pore size distributions of MCM-48 supported catalysts should have definite advantages.

Therefore, the MCM-48 supported chromium catalysts developed in this work could be very interesting if these catalysts are used in the adsorption/catalysis dual function system, similar to those developed by Greene and coworkers [1–3]. The high surface area, large and unique pore size, transition metal active sites, and potentially tunable surface properties (e.g., acidic and hydrophobic/hydrophilic properties) of the mesoporous M41S materials should provide great potentials for environmental application, such as the adsorption/catalysis process for the oxidative destruction of CVOC.

## 4. Conclusions

A Cr/MCM-48 catalyst has been successfully synthesized. $N_2$ adsorption/desorption and XRD characterization confirmed that the mesoporous structural properties of the catalyst are maintained upon loading of ~3 wt% of Cr onto the catalyst. TGA/DTA data identified the possible interactions of the templated surfactant molecule with chromium species, suggesting the possible incorporation of chromium into the mesoporous structure of the catalyst. Cr/MCM-48 catalysts showed excellent catalytic activity (100% conversion at 350°C) and catalytic stability (stable for 72 h) for the oxidative destruction of TCE. Cr/MCM-48 catalyst has high adsorption capacity for TCE (>0.25 g of TCE/g catalyst). Furthermore, the hydrophobicity of Cr/MCM-48 catalysts was shown to be increased using silica as the main framework composition.

## Acknowledgements

Funding from Environmental Technology Enterprise for this project is acknowledged with appreciation. The authors are also grateful to Shimadzu (Singapore) for allowing to use the XRD facility in their service center.

## References

[1] H.L. Greene, D.S. Prakash, K.V. Athota, Appl. Catal. B 7 (1996) 213.
[2] H.L. Greene, D. Prakash, K. Athota, G. Atwood, C. Vogel, Catal. Today 27 (1996) 289.
[3] D.S. Prakash, K.V. Athota, H.L. Greene, Novel adsorbents and their environmental applications, AIChE Symp. Series 91 (1995) 1.
[4] B. Ramachandran, H.L. Greene, S. Chatterjee, Appl. Catal. B 8 (1996) 157.
[5] R.S. Drago, S.C. Petrosius, G.C. Grunewald, W.H. Brendly Jr., in: J.N. Armor (Ed.), Environmental Catalysis, ACS Symposium Series, Denver, CO, 28 March–2 April 1993, Washington, DC, 1994, p. 340.
[6] S.C. Petrosius, R.S. Drago, V. Young, G.C. Grunewald, J. Am. Chem. Soc. 115 (1993) 6131.
[7] L. Storaro, R. Ganzerla, M. Lenarda, R. Zanoni, J. Mol. Catal. A 97 (1995) 139.
[8] X.-Z. Jiang, L.-Q. Zhang, X.-H. Wu, L. Zheng, Appl. Catal. B 9 (1996) 229.
[9] F. Solymosi, J. Rasko, E. Papp, A. Oszko, T. Bansagi, Appl. Catal. A 131 (1995) 55.
[10] S. Chatterjee, H.L. Greene, J. Catal. 130 (1991) 76.
[11] C. Kresge, M.E. Leonowicz, W.J. Roth, J.C. Vartuli, J.S. Beck, Nature 359 (1992) 710.
[12] R. Schmidt, H. Junggreen, M. Stocker, Chem. Commun. 875 (1996).
[13] D. Schmidt, D. Akporiaye, M. Stocker, O.H. Ellestad, Stud. Surf. Sci. Catal. 84 (1994) 61.